Maximum Likelihood Image Reconstruction using Data Fusion between X-Ray and Microwave Radar

Matthew T. Tivnan, Carey M. Rappaport

***Abstract*—**

Data fusion is the process by which measurements collected by two or more sensors are combined to produce a better result than could have been produced by any of the sensors acting individually. X-ray transmission and Microwave Tomography (MWT) are good candidates for data fusion because of their complementary strengths. For example, X-Ray is known for high spatial resolution structural imaging and MWT provides higher contrast in the physical properties for certain applications. In this work, a simple image reconstruction algorithm is presented which utilizes data fusion between X-Ray and MWT measurements. One possible application in neuroimaging is then simulated in a numerical experiment. The final results show that data fusion has significant advantages over conventional approaches.

I. INTRODUCTION

Imaging and reconstruction from indirect measurements is an important issue in science and engineering research with applications in non-destructive testing of materials, airport security, and medical imaging among others. Great technological strides have been made for individual imaging modalities; however, improvements are still possible through data fusion. The goal of the fused approach is to reconstruct an object using data gathered through two or more different physical processes. Data fusion is considered successful if the fused image provides more information than the images generated by the contributing modalities acting individually. Moving forward, there would be no requirement that novel imaging modalities are superior to existing methods; through data fusion, any new information can contribute to an improved image. Small changes in the quality of an image can often contain dramatically important new information.

In this work, data fusion using X-ray Computed Tomography (CT) and Microwave Tomography (MWT) measurements for image reconstruction will be considered. X-ray is one of the earliest forms of imaging and remains to this day as the so-called “gold-standard”, especially when it comes to interfaces between two different types of tissue. The absorption of X-rays as they pass through biological tissue can be accurately modeled as a linear process, which makes image processing simple. CT involves the rotation of sensors around the object under test and the collection of X-ray projections at each of the angles, known as a view, to form a complete dataset known as a sinogram. The structure of the image is related to the sinogram through a mathematical process known as the Radon transform. It can therefore be extracted using the associated inverse process which is known as filtered back-projection. However, X-ray imaging has certain drawbacks, including the relatively low radiological contrast between different types of tissues. Two completely different types of tissues which happen to have the same density can often be indistinguishable. In addition, CT scans deposit harmful radiation. Exposure to radiation can be reduced by decreasing the number of CT views or by reducing the intensity per view – both of which decrease the quality of the final image. A high-quality image may be possible using low-radiation X-ray measurements through data fusion with another modality.

Microwave Tomography is an emerging medical imaging modality in which the tissue is probed by a microwave electromagnetic wave. The electromagnetic field which is scattered by the tissue is then measured and used to image the hidden structure. In certain applications, the contrast in the dielectric properties of different materials is higher than the radiological contrast of X-ray, and the radiation is generally considered benign because it is non-ionizing. However, MWT has poor spatial resolution; objects that are small relative to the wavelength of the interrogating electromagnetic wave are often difficult or impossible to resolve. Additionally, the inverse problem, which is to reconstruct the object given the measured scattered electromagnetic field, is known to be ill-posed. To address this issue, there is a science and an art to the optimal arrangement of antennas and the constraint of possible solutions; however, imaging and reconstruction using MWT is usually very difficult.

Data fusion between these two modalities aims to combine the high resolution of X-ray and the high contrast of MWT in a single reconstruction algorithm. In certain applications, fusion can lead to a higher tolerance to noise. In other cases, it can actually extract information which was previously unavailable to either of the sensors acting individually. For these reasons, there has recently been much attention paid to hybrid CT-MWT imaging [1-2].

In the opening sections of this work, the physical and mathematical justifications are derived for a maximum likelihood data fusion algorithm. The algorithm is then described in full for a general case such that it can be applied to many situations and configurations. In the final section, a specific example is explored in depth in a numerical experiment. The chosen application is Neuroimaging for detection of carcinoma.

II. Sensor Descriptions

A. X-Ray Computed Tomography

In order to simulate the measurements collected by a CT scanner, a computational model is designed based on an understanding of X-ray physics. A parallel beam configuration, as shown in Fig. 1 will be considered.

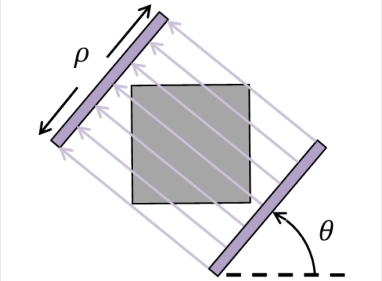

Fig. 1. Configuration for parallel beam X-ray CT. X-ray sources and detectors are shown in violet. View angle and ray position are annotated.

As X-rays propagate, their energy is absorbed based on the characteristic properties of the object under test. This attenuation of intensity is described by

$$I(\rho,\theta) = I_0 e^{-g(\rho,\theta)} \tag{1}$$

where $I(\rho,\theta)$ is the intensity of an X-ray after it passes through the object under test, I_0 is the initial intensity, and $g(\rho,\theta)$ is the distribution of accumulated attenuation which is sometimes referred to as a sinogram, and is given by

$$g(\rho,\theta) = \int_{L_{\rho,\theta}} \mu(x,y)\cdot dl \tag{2}$$

where $L_{\rho,\theta}$ is the linear path followed by the X-ray, and μ is the distribution of mass attenuation coefficients for the object under test. Equation (1) requires that g be a unitless quantity, so μ is given in units of cm^{-1}. This transformation from (x,y) space to (ρ,θ) is called the Radon transform. A discrete version of this integral transformation is easily found by replacing the integral with a summation, and estimating $\mu(x,y)$ by interpolation from sampled distribution

The measured quantity in X-ray imaging is the intensity, I. Measurement noise is often normally distributed and referred to as additive Gaussian white noise (AWGN). It is typically identically distributed with respect to intensity. However, the initial transmitted intensity I_0 can be adjusted so that pseudo-measurements of g have identically distributed AWGN, which is much more convenient for most imaging algorithms. The effective measurement array is therefore given by

$$\overline{y_{CT}} = \bar{g} + \overline{z_{CT}} \tag{3}$$

where $\overline{y_{CT}}$ contains the CT measurements, and $\overline{z_{CT}}$ contains independent identically distributed zero-mean AWGN with known variance, σ_{CT}^2. The arrays are equal in length and have one element for each X-ray detector.

B. Microwave Tomography

In MWT, electromagnetic waves cannot be accurately modeled as rays passing through the object under test. Instead, one must consider an interdependent network of scattered and re-scattered electromagnetic fields. The amplitude and phase of the total field is measured by the receiving antennas. A typical configuration for MWT is shown in Fig. 2.

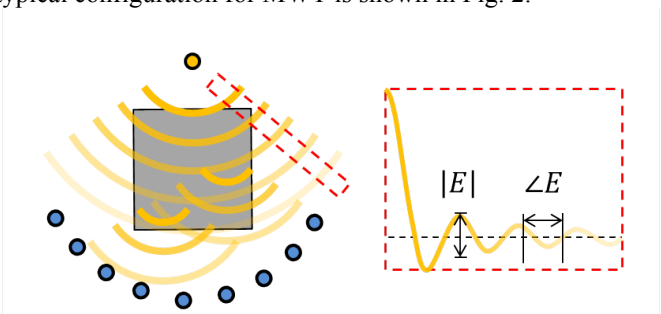

Fig. 2. Configuration for MWT. Transmitter shown in gold, receivers shown in blue. Amplitude and phase are annotated in the red break-out box.

A 2D case with the magnetic field oriented in the transverse direction will be considered. In this configuration, the electric field integral equation can be written as

$$E(x,y) = E^0(x,y) + \int\int G(x,y,x',y')J(x',y')dx'dy' \tag{4}$$

where E is the total electric field, E^0 is the incident electric field which depends on the transmitting antennas, and G is the Green's function which describes the response for all positions to a small change in the current density J, which is defined as

$$J(x,y) = \chi(x,y)E(x,y) \tag{5}$$

where χ is the dielectric contrast. The ultimate goal of MWT is to reconstruct χ by measuring E. Notice that equation (4) defines E in terms of J and equation (5) defines J in terms of E. This structure is characteristic of a non-linear inverse problem – that is, E cannot be written as a linear transformation of χ, and there is therefore no inverse linear system which would allow for the direct reconstruction of χ from measurements in E collected by receiving antennas. However, computational models such as Finite Difference Frequency Domain (FDFD) are able to find an accurate solution for E given χ and E_0.

The receiving antennas which collect the electric field introduce AWGN. The measurement array can therefore be written as by

$$\overline{y_{MWT}} = \bar{E} + \overline{z_{MWT}} \tag{6}$$

where $\overline{y_{MWT}}$ contains the MWT measurements, and $\overline{z_{MWT}}$ contains independent identically distributed zero-mean AWGN with known variance, σ_{MWT}^2. The arrays are equal in length and have one element for each receiving antenna.

III. Algorithm Description

A. Maximum Likelihood Detection in AWGN

In general, measurements collected in the presence of AWGN can be described by the following formula:

$$\bar{y} = \bar{x} + \bar{z} \tag{7}$$

where $\bar{y}$ is an array which contains the measurements, $\bar{x}$ is the signal of interest, and $\bar{z}$ contains independent identically distributed AWGN with known variance of σ_z^2.

In Maximum Likelihood detection, there must be some finite number M of possible signals. After the measurements are collected, the goal is to simply find the signal x_m which is most likely to produce the measured data. The optimization problem can be formally written as

$$\max_m \; P(\bar{x} = \overline{x_m} \mid \bar{y}) = \max_m \; P(\bar{z} = \bar{y} - \overline{x_m}) \tag{8}$$

Here, notation is borrowed from probability theory. For example, $P(A|B)$ is the probability that event A will occur given that event B has occurred, and $\max_m C_m$ evaluates to the index m for which C_m of the finite set $\bar{C}$ is maximum.

If $\bar{y}$, $\bar{x}$, and $\bar{z}$ each have K elements, then the joint event inside the probability operator in equation (8) can be rewritten in terms of a union between events for each individual sensor as follows:

$$\max_m P\left(\bigcup_{k=1}^{K} z_k = y_k - x_{m,k}\right) \tag{9}$$

Here, capital "U" notation is used to indicate a repeated union of events (event D_1 AND event D_2 AND … event D_K). The noise for any given sensor is independent of the noise for any other sensor, so by the definition of independence, the optimization problem can be rewritten as

$$\max_m \prod_{k=1}^{K} P\left(z_k = y_k - x_{m,k}\right) \tag{10}$$

Here, capital pi notation is used to represent a repeated product. The random variable z_k has a Gaussian distribution with zero-mean and variance σ_z^2. Substituting the general form for a Gaussian distribution leads to

$$\max_m \prod_{k=1}^{K} C_0 e^{-\frac{1}{2\sigma_z^2}\left|y_k - x_{m,k}\right|^2} \tag{11}$$

$$\max_m \left(C_0 e^{\frac{1}{2\sigma_z^2}}\right)^K \prod_{k=1}^{K} e^{-\left|y_k - x_{m,k}\right|^2} \tag{12}$$

where C_0 is simply a normalizing constant so that the sum of the probabilities of all possibilities is equal to 1.

The next few steps in the derivation require the utilization of special properties of the maximization operator. The relevant identities are listed below:

$$\max_m x_m = \max_m \; \alpha x_m \tag{13}$$

$$\max_m x_m = \max_m \; \ln x_m \tag{14}$$

$$\max_m x_m = \min_m -x_m \tag{15}$$

The first identity shows that maximization of a quantity is equivalent to the maximization of a quantity times any constant α. The second shows that the maximization of a quantity is the same as the maximization of a logarithm of the same quantity, since the logarithm is a monotonically increasing function. Lastly, finding a maximum of a quantity is the same as finding the minimum of its opposite.

Using the identity in (13), the constant outside the repeated product in (11) can be eliminated.

$$\max_m \prod_{k=1}^{K} e^{-\left|y_k - x_{m,k}\right|^2} \tag{16}$$

Taking the logarithm of the maximization operand as described in (14) and simplifying leads to

$$\max_m \; \ln\left(\prod_{k=1}^{K} e^{-\left|y_k - x_{m,k}\right|^2}\right) \tag{17}$$

$$\max_m \sum_{k=1}^{K} \ln\left(e^{-\left|y_k - x_{m,k}\right|^2}\right) \tag{18}$$

$$\max_m \sum_{k=1}^{K} -\left|y_k - x_{m,k}\right|^2 \tag{19}$$

Finally, using the identity in (15) gives

$$\min_m \sum_{k=1}^{K} \left|y_k - x_{m,k}\right|^2 \tag{20}$$

This is the end of the derivation and the final form of the optimization problem. The solution is chosen as the signal $\overline{x_m}$ which leads to the lowest sum of squared residuals with respect to the measurements. This process is commonly referred to as minimizing the least-squared cost function.

$$\mathcal{J}_m = \sum_{k=1}^{K} \left|y_k - x_{m,k}\right|^2 \tag{21}$$

B. Data Fusion Algorithm

Applying Maximum Likelihood detection to CT and MWT is straight-forward. A finite set of M possible solutions is generated, each corresponding to certain distributions of mass attenuation coefficients $\mu_m(x,y)$ and dielectric contrasts $\chi_m(x,y)$. Next, the signal $g_m(\rho,\theta)$ is generated via the Radon transform, and the signal $E_m(x,y)$ is generated via FDFD. These hypothesized signals are compared to the measurements $\overline{y_{CT}}$ and $\overline{y_{MWT}}$ using a pair of least-squared cost functions.

$$\mathcal{J}_{CT,m} = \sum_{k=1}^{K_{CT}} \left| y_{CT,k} - g_{m,k} \right|^2 \tag{22}$$

$$\mathcal{J}_{MWT,m} = \sum_{k=1}^{K_{MWT}} \left| y_{MWT,k} - E_{m,k} \right|^2 \tag{23}$$

In this framework, data fusion is simple – the fused cost function for the algorithm is defined as

$$\mathcal{J}_m = \mathcal{J}_{CT,m} + \beta \mathcal{J}_{MWT,m} \tag{24}$$

where β is a heuristically chosen constant which weights the relative impacts of CT and MWT. The optimal solution is chosen as the one which results in the lowest fused cost. A flowchart representation of the full algorithm is shown below.

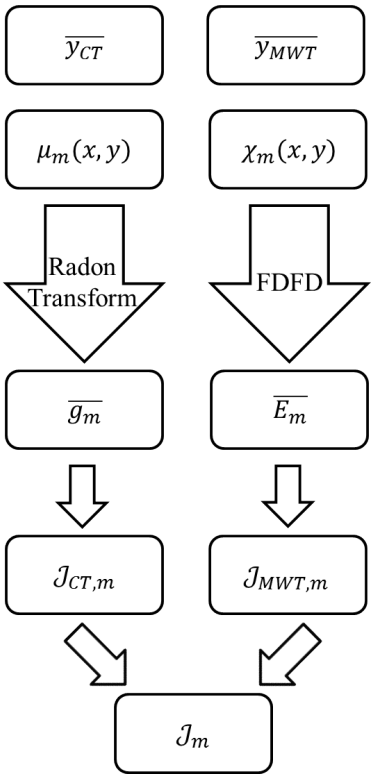

Fig. 3. Flow chart for complete maximum likelihood data fusion algorithm

IV. Application: NeuroImaging

In this numerical experiment, a neuroimaging configuration will be considered. A tumor with a known center but unknown radius and material

A simplified two-dimensional lossless configuration is considered based on an axial scan where the region of interest is composed of homogeneous sub-regions made up of either bone, carcinoma, cerebral spinal fluid (CSF), white matter, gray matter, or air. A single view at 0 degrees is used for CT and a single operating frequency of 1GHz is used for MWT.

A six-month check-up on a previously detected presence of brain carcinoma will be considered. For a certain fictitious clinical subject, a healthy baseline scan was collected 3 years ago, as well as a scan from six months ago which shows a circular brain carcinoma with a radius of 50mm. In the past six months, treatment has led to a decrease in the size of the tumor and it is now 25mm in radius. Measurements are simulated using the Radon transform and FDFD forward models and adding AWGN such that the signal to noise ratio is 30dB for each sensor. It is the task of the data fusion algorithm to reconstruct this tissue type and radius of a circular region which has the same center as the carcinoma in the six month old scan using the CT and MWT measurements.

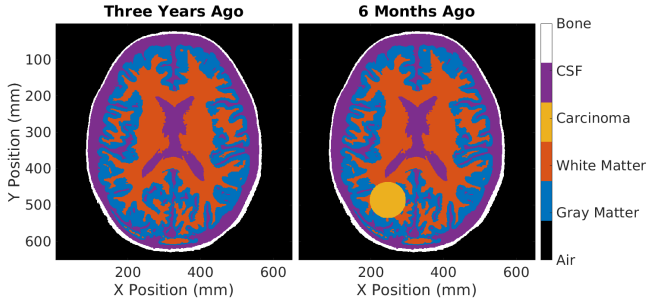

Fig. 4.Final results from previous scans. These are treated as prior knowledge.

Each material has characteristic mass attenuation coefficients and dielectric constants. Data from [3] are used for mass attenuation coefficients and data from [4] and [5] are used to define dielectric properties. The material properties of each material are shown in the figure below.

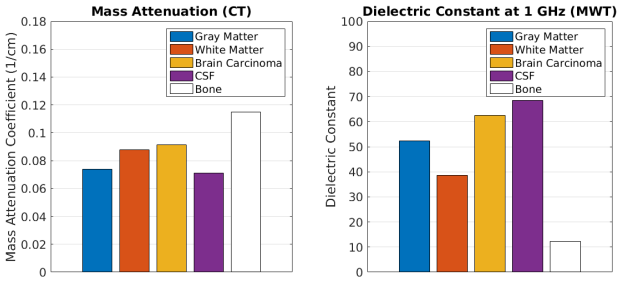

Fig. 5. Relevant mass attenuation coefficients and dielectric constants

The finite set of M possible solutions is generated by inserting a circular region at a given center point into the healthy image from the three year old scan. Radii between 0 and 50 mm,

mass attenuation coefficients between 0.07 and 0.12 cm^{-1} , and dielectric constants between 50 and 80 are considered. This solution set corresponds to a 3 dimensional parameter space. The CT-based cost function will depend on the radius and the mass attenuation coefficient of the circular region, the MWT-based cost function will depend on the radius and dielectric constant, and the fused cost function will depend on all three parameters. For each possible case, the signals $\overline{g_m}$ and $\overline{E_m}$ are computed using the Radon transform and FDFD, respectively. The resulting CT-based and MWT-based cost functions are shown in the contour plot below.

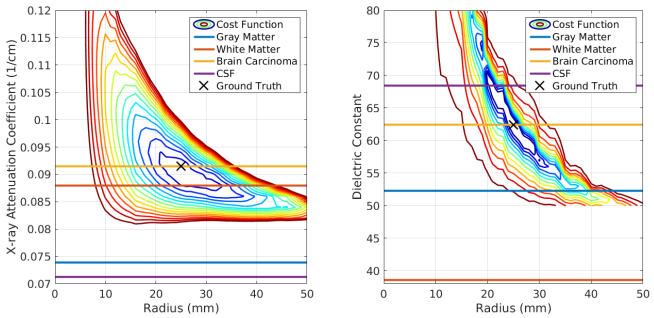

Fig. 6. CT-based and MWT-based cost function contour plots. The region inside the innermost blue contour corresponds to the most likely cases.

The CT-based cost function is lowest for brain carcinoma and white matter, and the MWT-based cost function is lowest for brain carcinoma and CSF. It is already clear that brain carcinoma is the only overlap between possible solutions yielded by the two sensors.

The fused cost function is then evaluated for all possible solutions. The weighting parameter β is chosen such that the each sensor type has the same impact on the solution – that is, the lowest occurrence in each cost function is normalized to the same value. The final results are shown in the figures below

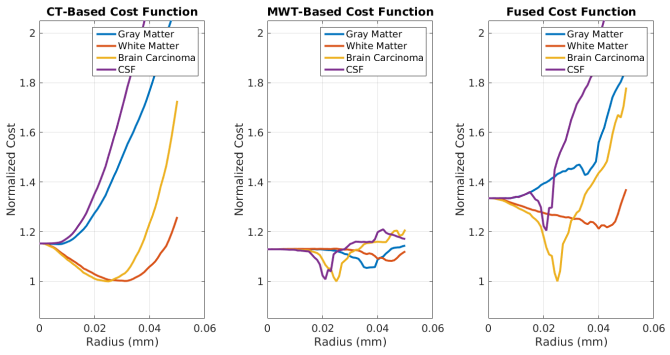

Fig. 7. CT-based, MWT-based and Fused cost functions plotted vs. radius.

Figure 7 shows that the CT-based and MWT-based cost functions are insufficient on their own. However, the fused cost function has a clear minimum for brain carcinoma with a radius of 25mm – the correct solution.

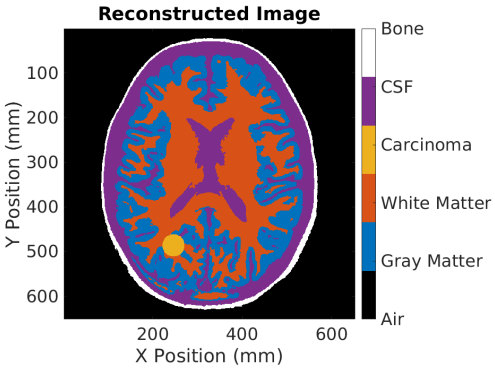

Fig. 8. Reconstructed image showing the carcinoma with a radius of 25mm

V. Conclusion

Figure 6 shows that neither modality is able to completely isolate the correct solution acting individually. However, the two methods contain complimentary information which is exploited by the data fusion algorithm. In the end, the correct image is reconstructed as shown in Figures 7 and 8. The numerical experiment serves as an example of the advantages offered by data fusion. In this case, information was extracted through data fusion which would not have been available using either modality individually.

VI. Perspective Application: Airport Security

The same process may also have applications in airport security screening if microwave radar and x-ray CT measurements are both collected. Currently airport security CT scanners rely on image processing algorithms applied to the final imaging result to detect threats. If however, MWT sensors could be incorporated, threats could be detected automatically based on their material properties.

Acknowledgment

Financial support for this work was provided by the Department of Homeland Security Science and Engineering Workforce Development Program.

References

[1] M. Tivnan, C. Rappaport, J. Martinez-Lorenzo, A. Morgenthaler. (2014, April) FDFD Microwave Modeling of Realistic, Inhomogeneous Breast Tissue Based on Digital Breast Tomosynthesis Priors for Cancer Detection. Presented at Northeast Bioengineering Conference. Print.

[2] M. Tivnan, A. Morgenthaler, J. Martinez-Lorenzo, R. Moore, C. Rappaport. (2015, March). Fusion of Digital Breast Tomosynthesis and Microwave Radar Imaging for a High Contrast Breast Cancer Imaging Algorithm. Presented at URSI Journees Scientifiques. Print.

[3] ICRU "Tissue Substitutes in Radiation Dosimetry and Measurement", Report 44 of the International Commission on Radiation Units and Measurements Bethesda, MD, 1989

[4] C. Gabriel, "Compliation of The Dielectric Properties of Body Tissues at RF and Microwave Frequencies," Occ. and Env. Health Directorate, Brooks Air Force Base, TX, Rep., 1996.

[5] Y. Done-Sik, K. Bong-Seok, C. Hyung-Do, L. Ae-Kyoung, P. Jeong–Ki. October 2004. Dielectric Properties of Carcinomas. *Bioelectromagnetics.* Print. *Volume 25 (issue 7),* pages 492–497, Available: site/path/file

STUDENT BIO: MATT TIVNAN

Matt Tivnan is a Senior at Northeastern University pursuing a combined degree in Electrical Engineering and Physics. He has conducted advanced imaging research for four years with a focus on Microwave Radar Imaging in biological tissues. His co-ops have included the École Supérieure d'Electricité in Paris, France where he developed extensions to his undergraduate research and PhotoDiagnostic Systems in Boxboro, MA where he helped design and build CT and PET scanners. Matt is a mentor in the Gordon Scholars program, a COE mentor in the first-year program, a Community Outreach Officer for the IEEE student chapter, and a member of the ALERT student leadership counsel. He is also the first recipient of the undergraduate fellowship sponsored by the Department of Homeland Security Science and Engineering Workforce Development Program. Matt plans to pursue a graduate education and a career in the field of advanced medical imaging technology.